

SIMULATION AND ANALYSIS OF TIBC FOR INDUCTION MOTOR DRIVE

A.Mythily¹, N.P.Ananthamoorthy²

¹PG Scholar, Department of EEE, Hindusthan college of Engineering and Technology

²Head Of the Department, Department of EEE, Hindusthan college of Engineering and Technology

Abstract-This project proposes a new low cost converter- inverter drive system for induction motor. The converter is designed to drive a three-phase induction motor directly from PhotoVoltaic (PV) energy source. The three phase induction motor is better because of its low cost, reliability, no maintenance, high efficiency and good power factor. Two Inductor Boost Converter (TIBC) is used in first stage along with the voltage doubler rectifier and snubber to develop the system. The reason to choose TIBC is due to its high voltage gain and low input current ripple, which minimizes the oscillations at the module operation point. To convert the boosted DC output voltage from PV module into AC, a voltage source inverter is implemented to attain sufficient voltage to drive the motor. As the PV cell poses the nonlinear behaviour, the Maximum Power Point Tracker (MPPT) controller is needed to improve the utilization efficiency of the converter. The MPPT algorithm proposed in this paper based on hill climbing algorithm, for matching the load and to boost the PV module output voltage. PI Controller is used to control the speed of the Induction Motor. The entire system is simulated using Matlab Simulink environment. The system is expected to be operated with high efficiency and low cost for long lifetime.

Keywords- Induction Motor, Photovoltaic Source, Two Inductor Boost Converter (TIBC), Three Phase Voltage Source Inverter (VSI), Proportional Integral Controller (PI).

I. INTRODUCTION

CURRENTLY, over 900 million people in various countries do not have drinkable water available for consumption. Of this total, a large amount is isolated, located on rural areas where the only water supply comes from the rain or distant rivers [1]. This is also a very common situation in the north part of Brazil, where this work was developed. In such places, the unavailability of electric power rules out the pumping and water treatment through conventional systems. One of the most efficient and promising way to solve this problem is the use of systems supplied by photovoltaic (PV) solar energy. This kind of energy source is becoming cheaper and has already been put to work for several years without the need of maintenance. Such systems are not new and are already used for more than three decades [1]. Nevertheless, until recently, the majority of the available commercial converters in Brazil are based on an intermediate storage system, performed with the use of lead-acid batteries, and dc motors to drive the water pump [3]. More sophisticated systems have already been developed with the use of a low-voltage synchronous motor [4], but these, although presenting higher efficiency, are too expensive to be used in poor communities that need these systems.

The batteries allow the motor and pump system to always operate at its rated power even in temporary conditions of low solar radiation. This facilitates the coupling of the electric dynamics of the solar panel and the motor used for pumping [5]. Generally, the batteries used in this type of system have a low life span, only two years on average [5], which is extremely low compared to the

useful life of 20 years of a PV module. Also, they make the cost of installation and maintenance of such systems substantially high. Furthermore, the lack of battery replacement is responsible for the failure of such systems in isolated areas. The majority of commercial systems use low-voltage dc motors, thus avoiding a boost stage between the PV module and the motor [7]. Unfortunately, dc motors have lower efficiency and higher maintenance cost compared to induction motors and are not suitable for applications in isolated areas, where there is no specialized personnel for operating and maintaining these motors. Another problem is that low-voltage dc motors are not ordinary items in the local markets. Because of the aforementioned problems, this work adopted the use of a three phase induction motor, due to its greater robustness, lower cost, higher efficiency, availability in local markets, and lower maintenance cost compared to other types of motors.

The design of a motor drive system powered directly from a PV source demands creative solutions to face the challenge of operating under variable power restrictions and still maximize the energy produced by the module and the amount of water pumped [8]. These requirements demand the use of a converter with the following features: high efficiency—due to the low energy available; low cost—to enable its deployment where it is most needed; autonomous operation—no specific training needed to operate the system; robustness—minimum amount of maintenance possible; and high life span—comparable to the usable life of 20 years of a PV panel. This paper proposes a new dc/dc converter and control suitable for PV water pumping and treatment that fulfill most of the aforementioned features. This paper is organized as follows. In Section II, the proposed system is described. In Section III, the dc/dc converter itself is presented and analyzed. In Section IV, the control strategy is explained, and in Section V, the experimental results are presented.

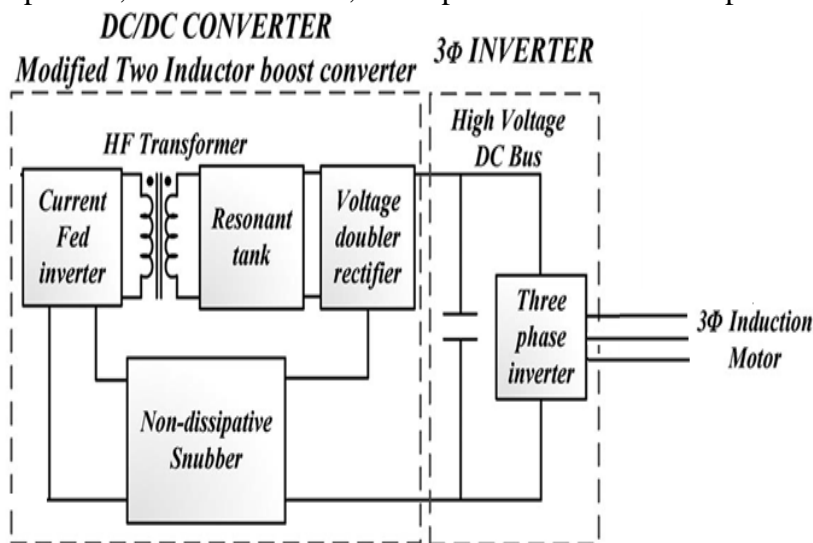


Figure 1. Simplified block diagram of the proposed system

II. PROPOSED SYSTEM

To ensure low cost and accessibility of the proposed system, it was designed to use a single PV module. The system should be able to drive low-power water pumps, in the range of 1/3 hp, more than enough to supply water for a family. Fig. 1 presents an overview of the proposed system. The energy produced by the panel is fed to the motor through a converter with two power stages: a dc/dc two-inductor boost converter (TIBC) stage to boost the voltage of the panels and a dc/ac three-phase inverter to convert the dc voltage to three-phase ac voltage. The inverter is based on a classic topology (three legs, with two switches per leg) and uses a sinusoidal pulse width modulation (PWM) (SPWM) strategy with 1/6 optimal third harmonic voltage injection as proposed in [9]. The use of

this PWM strategy is to improve the output voltage level as compared to sinusoidal PWM modulation. This is a usual topology, and further analyses on this topology are not necessary. For the prototype used to verify the proposed system, a careful selection of the voltage source inverter (VSI) components is more than enough to guarantee the efficiency and cost requirements. The required dc/dc converter for this kind of system needs to have a large voltage conversion ratio because of the low-voltage characteristic of the PV panels and small input current ripple so that it does not cause oscillation over the maximum power point(MPP) of the PV module [10]–[12], thus ensuring the maximum utilization of the available energy. The commonly used isolated voltage-fed converters normally have a high input current ripple, which forces the converter to have large input filter capacitors.

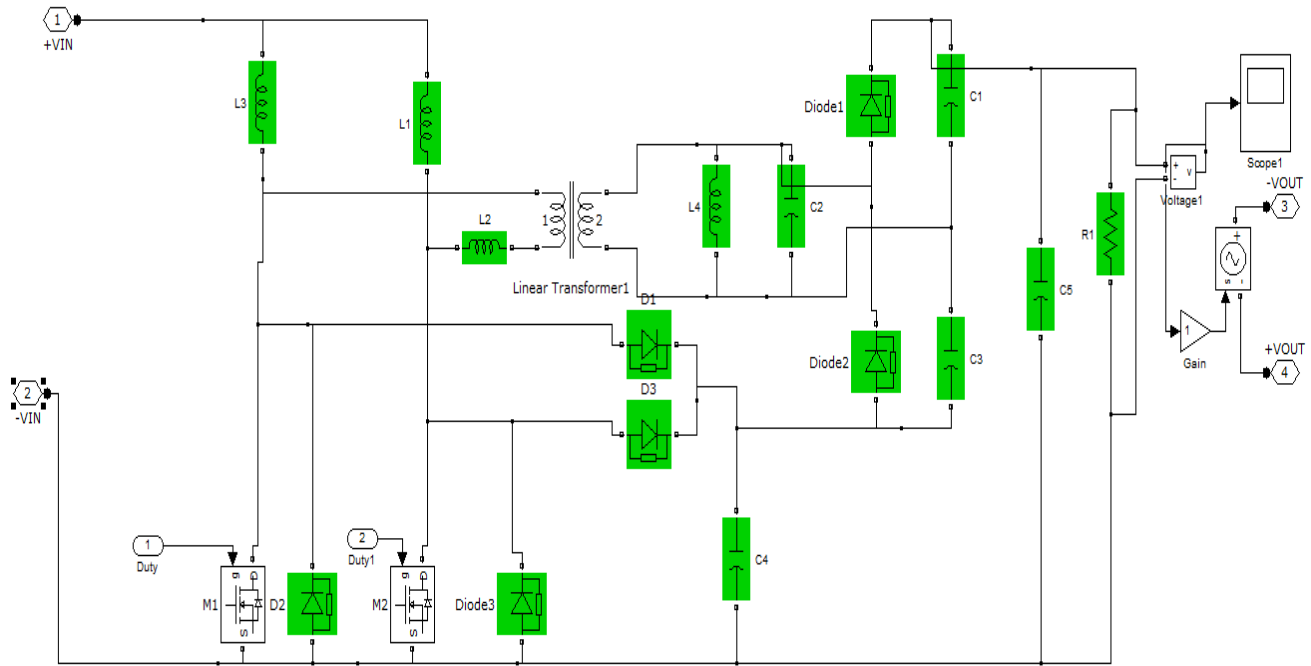


Figure 2. Modified TIBC topology

These are normally electrolytic, which are known to have a very small lifetime and thus affect the overall life span and mean time before failure of the converter. Furthermore, the inherent step-down characteristic of the voltage-fed converters, the large transformer turns ratio needed to boost the output voltage, the high output diode voltage stress, and the need of an LC output filter [13] make voltage-fed converters not the best choice for this application.

When compared to the voltage-fed topologies, current-fed converters have some advantages. Usually, they have an inductor at the input, so the system can be sized to have input current ripple as low as needed, thus eliminating the need of the input capacitor at the panel voltage. Current-fed converters are normally derived from the boost converter, having an inherent high step-up voltage ratio, which helps to reduce the needed transformer turns ratio. The classical topologies of this kind are the current-fed push-pull converter [14], [15], the current-fed full-bridge [16], and the dual half-bridge converter [17]. Although the current-fed topologies have all the aforementioned advantages, they still have problems with high voltage spikes created due to the leakage inductance of the transformers and with high voltage stress on the rectifying diodes [18].

One of the solutions to the current-fed PWM converters is the use of resonant topologies able to utilize the component parasitic characteristics, such as the leakage inductance and winding capacitance of transformers, in a productive way to achieve zero current switching (ZCS) or zero

voltage switching (ZVS) condition to the active switches and rectifying diodes [19]. In this paper, the use of a modified TIBC for the first-stage dc/dc converter is proposed, due to its very small number of components, simplicity, high efficiency, easy transformer flux balance [20], [21], and common ground gate driving for both switches. These features make it the ideal choice for achieving the system's necessary characteristics. Aside from the high dc voltage gain of the TIBC, it also compares favorably with other current-fed converters concerning switch voltage stress, conduction losses, and transformer utilization [22], [23].

In addition, the input current is distributed through the two boost inductors having its current ripple amplitude halved at twice the PWM frequency. This last feature minimizes the oscillations at the PV module operation point and makes it easier to achieve the MPP. In its classical implementation, the TIBC is a hard-switched overlapped pulse-modulated converter; this way, at least one of the switches is always closed, creating a conduction path for the input inductor current. Nevertheless, the TIBC can be modified to a multiresonant converter by adding a capacitor at the transformer's secondary winding [24], [25]. A multiresonant tank is formed by the magnetizing inductance of the transformer, its leakage inductance, and the added capacitor, as shown in Fig. 2. The intrinsic winding capacitance of the transformer is included in the resonant capacitor.

The regenerative snubber is formed by two diodes and a capacitor connecting the input side directly to the output side of the converter, as shown in Fig. 2. This makes it a nonisolated converter, which has no undesirable effect in the PV motor driver applications. The voltage over the MOSFETs is applied to a capacitor connected to the circuit ground, and the voltage of this capacitor is coupled in series with the output of the rectifier. This modification allows part of the energy to be transferred from the input directly to the output, through the snubber, without going through the transformer, reducing its size and improving even more the efficiency of the converter.

III. OPERATION PRINCIPLE

To simplify the analysis of the proposed converter, the following assumptions need to be true during a switching interval: The input inductors L_{i1} and L_{i2} are sufficiently large so that their current is almost constant; the capacitors C_{o1} , C_{o2} , and C_s are large enough to maintain a constant voltage; and the output capacitors C_{o1} and C_{o2} are much larger than C_r to clamp the resonant voltage. In the hard-switched operation of the TIBC, the two primary switches Q_1 and Q_2 operate at an overlapped duty cycle switching scheme to guarantee a conduction path for the primary inductor current. When both Q_1 and Q_2 are turned on, L_{i1} and L_{i2} are charged by the input energy.

When $Q_1(Q_2)$ is opened, the energy stored in $L_{i1}(L_{i2})$ is transferred to $C_{o1}(C_{o2})$ through the transformer and the rectifier diode $D_{o1}(D_{o2})$. Once the multiresonant tank is introduced, two different resonant processes occur: 1) When both switches are closed, the leakage inductance L_r participates along with capacitance C_r in the resonance at the primary current switching and current polarity inversion, allowing ZCS operation for the primary switches, and 2) during the conduction time interval (between t_4 and t_5 in Fig. 3), when at least one of the switches is open, L_r is associated in series with L_{i1} or L_{i2} , not participating on the transformer's secondary current resonance, formed only by L_m and C_r .

An extended description of multiresonant TIBC without the snubber is presented and analyzed in [24], resulting in a detailed mathematical modeling for both resonant processes during its operation. However, the analysis in [24] is based on several complex mathematical models, and consequently, the presented design method shows several dependent variables, which translates in a design methodology difficult to be implemented. In this paper, a simplified methodology based on the effect

of each resonant process, the resonant frequencies, and the switching frequency is applied. Spice simulations and a prototype are used to show that, despite the simplicity of the design methodology, the correct operation of the converter is guaranteed, particularly the soft switching of the primary switches for the whole operating load range. Although the resonant process affects the output voltage, depending on the resonant tank component values and the load, this can be neglected because of its small influence and complex effect.

There are three main aspects in the proposed converter's control: 1) During normal operation, a fixed duty cycle is used to control the TIBC MOSFETs, thus generating an unregulated high bus voltage for the inverter; 2) an MPP tracking (MPPT) algorithm is used along with a PI controller to set the speed of the motor and achieve the energy balance of the system at the MPP of the PV module; and 3) a hysteresis controller is used during the no-load conditions and start-up of the system. Each of these aspects is described in the following sections.

A. Fixed Duty Cycle Control

One of the most important control aspects of this system is the fact that it is possible to use an unregulated dc output voltage and a fixed duty cycle for the first-stage dc/dc converter. As a resonant converter, there are definite time intervals in the switching period for the resonance process to occur. By altering the duty cycle or the switching period to control the output voltage, the converter may no longer operate at ZCS condition. Therefore, the fixed duty cycle is used to overcome these design problems and ensure that the converter is going to operate in ZCS condition despite the input voltage or output load. The duty cycle was chosen to guarantee that the amount of transferred energy occurs during most part of the switching interval. Therefore, it is possible to transfer the same amount of energy with a smaller rms current. Therefore, the losses in the input inductors (L_{i1} and L_{i2}), in the MOSFETs ($Q1$ and $Q2$), and in the transformer are smaller. As a result, the efficiency of the converter improves. Fig. 3 shows the $I-V$ characteristic curves for a typical solar panel.

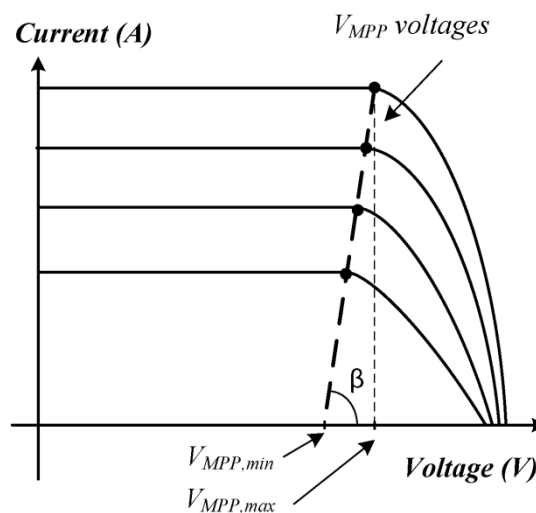


Figure 3 . $I-V$ characteristic curves for a typical solar panel.

B. MPPT Control

The MPPT is a strategy used to ensure that the operating point of the system is kept at the MPP of the PV panel [27]. The widely used hill-climbing algorithm was applied due to its simple implementation and fast dynamic response. This MPPT technique is based on the shape of the power curve of the PV panel. This curve can be divided into two sides, to the left and to the right of the MPP. By analyzing the power and voltage variation, one can deduce in which side of the curve the PV panel is currently operating and adjust the voltage reference to get closer to the desired point. The voltage reference is

used on a PI controller to increase or reduce the motor speed and consequently adjust the bus and panel voltage by changing its operating point.

C. Hysteresis Control

The main drawback of the classical TIBC is its inability to operate with no load or even in low-load conditions. The TIBC input inductors are charged even if there is no output current, and the energy of the inductor is lately transferred to the output capacitor raising its voltage indefinitely until its breakdown. Classically, the input MOSFET cannot be turned off because there is no alternative path for the inductor current. However, with the addition of the proposed snubber, the TIBC switches can be turned off. The main characteristics of the used panel and motor are shown in Table I. Thus, a hysteresis controller can be set up based on the dc bus voltage level. Every time a maximum voltage limit is reached, indicating a low-load condition, this mode of operation begins. In this case, the switches are turned off until the dc bus voltage returns to a normal predefined level. As a result, the switching losses are reduced during this period of time.

IV. SIMULATION AND EXPERIMENTAL RESULTS

The proposed converter was simulated on Matlab. Fig. 4 shows the schematics used for the first-stage TIBC. All parasitic series resistances were included in the transformer and capacitors. The control of the primary MOSFETs was simulated using a fixed pulse modulation and a voltage-controlled source to implement the hysteresis control within the limits of 380 V/ 10 V. Fig. 8 shows the overlapped pulses used to control $Q1$ and $Q2$, the current in both input inductors, and the current in the PV module. It is observed that each one of the inductors has a current ripple at the converter switching frequency and out of phase with each other; however, both currents are supplied by the PV module, and when they are analyzed together (IPV), a reduction in the ripple amplitude to half of the original ones is seen.

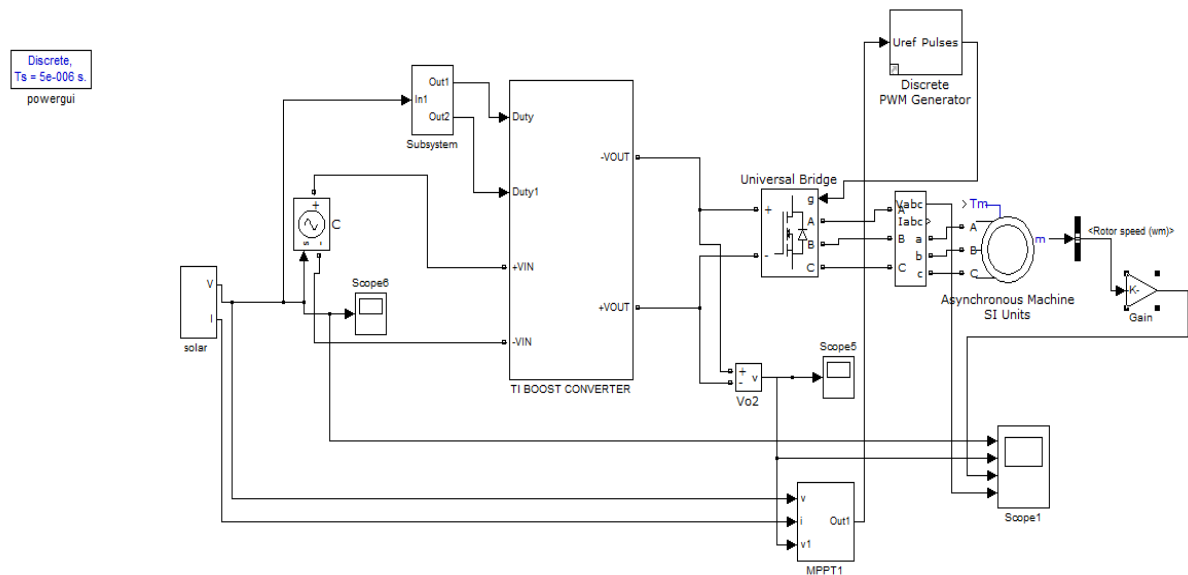


Figure 4. Circuit used in the simulation.

It is observed that there are no voltage spikes or increased voltage stress over the switches. In addition, the figure shows that both turn-on and turnoff occurs at almost ZCS. It is shown that not only the primary MOSFETs are operated under ZCS condition but also the rectifying diodes. The operation under ZCS condition allows the use of fast recovery diodes instead of the expensive silicon

carbide ones, thus reducing the total cost of the system. It was tested using real water pumping system and a PV module. A complete autonomous operation was obtained. This includes the system automatic start-up and shutdown according to the radiation level. A programmable source was used to emulate the solar radiation during the period of a day.

The converter was connected to this source to evaluate its overall performance. The system is supposed to operate on the MPP curves at all times, meaning that it needs to stay as close as possible to the green curves. These green curves are the MPPT voltage, current, and power levels produced by the programmable source. The system was able to operate near the ideal voltage (V_{MPP}) and current (I_{MPP}) during the programmed time, thus achieving operation close to the MPP. The generated power of the programmable source and the corresponding water flow for the same period of time are also shown. The MPPT routine analysis was also performed using a real PV module. A real time analysis of the operation point was done, i.e., the capability of keeping a steady position on the MPP of the PV panel. The system starts its operation at the open circuit voltage (VOC) and then stabilizes on the MPP. As the solar radiation varies, the MPPs move.

The system was able to stably track these points. The black dashed line shows all the points during a day. A maximum efficiency of 93.64% was obtained for the TIBC first stage dc/dc converter, and that of 91% was obtained for the complete system. These curves were obtained during a real operation with a PV panel, driving the water pump with varying solar radiation.

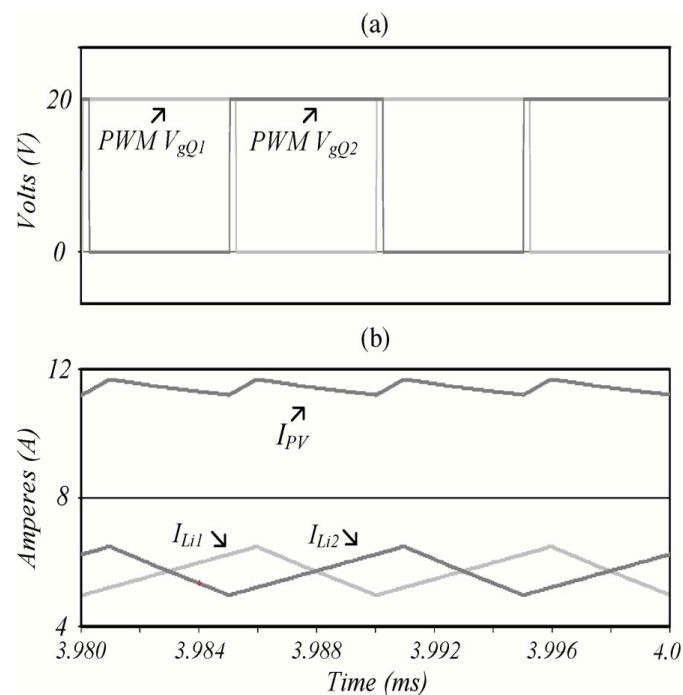


Figure 5. Simulation results of the input of the dc/dc converter. (a) Input switches' driving signals, (b) inductors' input currents I_{Li1} and I_{Li2} , and total input current (I_{PV}).

V. CONCLUSION

The proposed system describes a method in which a three phase motor is operated directly from the solar energy. In this method, the sunlight falling on the panel is undergone a number of mechanisms which makes it possible for the accurate working of the motor. The use of the TIBC converter reduces the component size and hence cost is also reduced. TIBC converter provides high voltage gain and will also reduce the input current ripple. Distributed conductivity of current proposed in this

method gradually reduces the copper loss. Better constant voltage control is gained by using this Hill Climbing algorithm along with PI controller than in other P&O methods. The future work is extended to be done by using the fuzzy logic controller.

REFERENCES

- [1] M. Chunting, M. B. R. Correa, and J. O. P. Pinto, "The IEEE 2011 international future energy challenge—Request for proposals," in *Proc. IFEC*, 2010, pp. 1–24.
- [2] A. Hahn, "Technical maturity and reliability of photovoltaic pumping systems," in *Proc. 13th Eur. Photovoltaic Solar Energy Conf.*, Nice, France, pp. 1783–1786. CARACAS
- [3] M. A. Vitorino and M. B. R. Correa, "High performance photovoltaic pumping system using induction motor," in *Proc. Brazilian Power Electron. Conf.*, 2009, pp. 797–804.
- [4] G. Teröde, K. Hameyer, and R. Belmans, "Sensorless control of a permanent magnet synchronous motor for PV-powered water pump systems using the extended Kalman filter," in *Proc. 9th Int. Conf. Elect. Mach. Drives*, 1999, pp. 366–370.
- [5] H. Harsono, "Photovoltaic water pump system," Ph.D. dissertation, Dept. Intell. Mech. Syst. Eng., Faculty Kochi Univ. Technol., Kochi, Japan, Aug. 2003.
- [6] D. Linden, *Handbook of Batteries and Fuel Cells*. New York, NY, USA: McGraw-Hill, 1984.
- [7] D. Tschanz, H. Lovatt, A. Vezzini, and V. Perrenoud, "A multi-functional converter for a reduced cost, solar powered, water pump," in *Proc. IEEE ISIE*, 2010, pp. 568–572.
- [8] M. A. Vitorino, M. B. R. Correa, C. B. Jacobina, and A. M. N. Lima, "An effective induction motor control for photovoltaic pumping," *IEEE Trans. Ind. Electron.*, vol. 58, no. 4, pp. 1162–1170, Apr. 2011.
- [9] S. R. Bowes and A. Midoun, "Suboptimal switching strategies for microprocessor controlled PWM inverter drives," *Proc. Inst. Elect. Eng.—Elect. Power Appl.*, vol. 132, no. 3, pp. 133–148, May 1985.
- [10] M. Cacciato, A. Consoli, and V. Crisafulli, "A high voltage gain dc/dc converter for energy harvesting in single module photovoltaic applications," in *Proc. IEEE ISIE*, 2010, pp. 550–555.
- [11] P. J. Wolfs, "A current-sourced dc-dc converter derived via the duality principle from the half-bridge converter," *IEEE Trans. Ind. Electron.*, vol. 40, no. 1, pp. 139–144, Feb. 1993.
- [12] P. Wolfs and Q. Li, "An analysis of a resonant half bridge dual converter operating in continuous and discontinuous modes," in *Proc. IEEE Power Electron. Spec. Conf.*, 2002, pp. 1313–1318.
- [13] W. Li, L. Fan, Y. Zhao, X. He, D. Xu, and B. Wu, "High step-up and high efficiency fuel cell power generation system with active clamp flyback forward converter," *IEEE Trans. Ind. Electron.*, vol. 59, no. 1, pp. 599–610, Jan. 2012.
- [14] T.-J. Liang, R.-Y. Chen, J.-F. Chen, and W.-J. Tzeng, "Buck-type current fed push-pull converter with ZCS for high voltage applications," in *Proc. IEEE Region 10 Conf.*, 2007, pp. 1–4.
- [15] P. M. Barbosa and I. Barbi, "A new current-fed, isolated PWM dc-dc converter," *IEEE Trans. Power Electron.*, vol. 11, no. 3, pp. 431–438, May 1996.
- [16] R.-Y. Chen, T.-J. Liang, J.-F. Chen, R.-L. Lin, and K.-C. Tseng, "Study and implementation of a current-fed full-bridge boost dc-dc converter with zero-current switching for high-voltage applications," *IEEE Trans. Ind. Appl.*, vol. 44, no. 4, pp. 1218–1226, Jul./Aug. 2008.
- [17] J. Kim, H.-S. Song, and K. Nam, "Asymmetric duty control of a dual-half-bridge dc/dc converter for single-phase distributed generators," *IEEE Trans. Power Electron.*, vol. 26, no. 3, pp. 973–982, Mar. 2011.
- [18] B. Liu, C. Liang, and S. Duan, "Design considerations and topology selection for dc-module-based building integrated photovoltaic system," in *Proc. 3rd IEEE Conf. ICIEA*, Jun. 3–5, 2008, pp. 1066–1070.
- [19] J. Biela and J. W. Kolar, "Using transformer parasitics for resonant converters—A review of the calculation of the stray capacitance of transformers," in *Conf. Rec. 40th IEEE IAS Annu. Meeting*, 2005, pp. 1868–1875.
- [20] L. Yan and B. Lehman, "Isolated two-inductor boost converter with one magnetic core," in *Proc. IEEE Appl. Power Electron. Conf. Expo.*, 2003, pp. 879–885.
- [21] Y. Jang, "Two-boost converter," U.S. Patent 6 239 584, May 29, 2001.
- [22] Q. Li and P. Wolfs, "The power loss optimization of a current fed ZVS two-inductor boost converter with a resonant transition gate drive," *IEEE Trans. Power Electronics*, vol. 21, pp. 1253–1263, Sep. 2006.
- [23] W. C. P. De Aragão Filho and I. Barbi, "A comparison between two current-fed push-pull dc-dc converters—Analysis, design and experimentation," in *Proc. INTELEC*, 1996, pp. 313–320.
- [24] B. Yuan, X. Yang, X. Zeng, J. Duan, J. Zhai, and D. Li, "Analysis and design of a high step-up current-fed multiresonant dc-dc converter with low circulating energy and zero-current switching for all active switches," *IEEE Trans. Ind. Electron.*, vol. 59, no. 2, pp. 964–978, Feb. 2012.
- [25] D. Li, B. Liu, B. Yuan, X. Yang, J. Duan, and J. Zhai, "A high step-up current fed multi-resonant converter with output voltage doubler," in *Proc. IEEE Appl. Power Electron. Conf. Expo.*, 2011, pp. 2020–2026.

- [26] Y. Jang and M. M. Jovanovic, "New two-inductor boost converter with auxiliary transformer," in Proc. IEEE Appl. Power Electron. Conf. Expo., 2002, pp. 654–660.
- [27] R. Faranda and S. Leva, "Energy comparison of MPPT techniques for PV systems," WSEAS Trans. Power Syst., vol. 3, no. 6, pp. 446–455, Jun. 2008.
- [28] KD 200-54 P Series Data Sheet, Kyocera Solar, Inc., San Diego, CA, USA, 2011.

